

DESIGN OF 162-MHz CW BUNCH-BY-BUNCH CHOPPER AND PROTOTYPE TESTING RESULTS*

A. Shemyakin[†], C. Baffes, J.-P. Carneiro, B. Chase, A. Chen, J. Einstein-Curtis, D. Frolov, B. Hanna, V. Lebedev, L. Prost, A. Saini, G. Saewert, D. Sun, Fermilab, Batavia, IL 60510, USA
D. Sharma, Raja Ramanna Center for Advanced Technology (RRCAT), India
C. Richard, Michigan State University, East Lansing, MI, USA

Abstract

The PIP-II program of upgrades proposed for the Fermilab accelerator complex is centered around an 800 MeV, 2 mA CW SRF linac. A unique feature of the PIP-II linac is the capability to form a flexible bunch structure by removing a pre-programmed set of bunches from a long-pulse or CW 162.5 MHz train, coming from the RFQ, within the 2.1-MeV Medium Energy Beam Transport (MEBT) section. The MEBT chopping system consists of two travelling-wave kickers working in sync followed by a beam absorber. The prototype components of the chopping system, two design variants of the kickers and a 1/4-size absorber, have been installed in the PIP-II Injector Test (PIP2IT) accelerator and successfully tested with beam of up to 5 mA. In part, one of the kickers demonstrated a capability to create an aperiodic pulse sequence suitable for synchronous injection into the Booster while operating at 500 V and average switching frequency of 44 MHz during 0.55 ms bursts at 20 Hz. This report presents the design of the PIP-II MEBT chopping system and results of prototypes testing at PIP2IT.

INTRODUCTION

In the coming decade, Fermilab plans to replace the existing linac with a new 800 MeV SRF H⁻ accelerator, a.k.a. PIP-II [1]. Presently, its first application is expected to be the injection into the Booster while later delivering a high-power beam simultaneously to multiple experiments. In the scheme proposed in [2] for the latter, a RF cavity with transverse field operating at a frequency of $(n+1/2)\times 162.5$ MHz (so-called RF splitter) placed downstream of the linac, distributes bunches to three channels according to the phase of their arrival. Since requirements for the beam time structure are likely to be very different for various experiments, the scheme suggested installing in the MEBT a dedicated fast chopping system (chopper) capable of removing individual bunches from initially true CW beam coming out of the 162.5 MHz RFQ. Only bunches fitting to the combined pattern of experiments' requests are passed for acceleration, while others are dumped within the MEBT.

Capability to create an arbitrary bunch pattern is beneficial for the scenario of the Booster injection as well. The fundamental bunch frequency of the PIP-II linac, 162.5 MHz, and the Booster frequency at injection, 44.7 MHz

are not harmonically related. In the bucket-to-bucket injection scenario described in [1], the chopper removes the bunches that would arrive at the boundaries of separatrix, creating an optimum longitudinal distribution and equal population of the Booster bunches. In addition, it creates a gap in the Booster bunches sequence to fire the extraction kicker at the end of the acceleration cycle.

The concept of the chopper as well as its prototype components were tested at the PIP-II Injector Test (PIP2IT, [3]) accelerator.

CHOPPER CONCEPT AND CHOICE OF PARAMETERS

The chopper consists of a set of electrostatic deflectors (kickers) and a beam absorber accepting the unwanted bunches. Bunch-by-bunch selection assumes that the kickers are capable of fully deflecting a "removed" bunch while perturbing minimally the neighbouring "passing" bunches. Full deflection is defined as separation of the passing and removed bunches in the transverse direction (chosen for PIP-II vertical and marked as Y in the text) by $6\sigma_y$, where σ_y is the vertical rms beam size at the absorber.

The deflection voltage pulse needs to travel along the kicker with the speed matching the velocity of the 2.1 MeV H⁻ ions, 20 mm/ns. Therefore, a corresponding travelling-wave structure is required.

The main parameters defining the scheme choices are the vertical emittance ($\sim 0.2 \mu\text{m rms n}$) and the achievable kicker plate voltage amplitude, i.e. difference of the voltage between states of passing and removing the bunches. The latter was chosen to be 500 V. Then, the minimum kicker gap was defined by the expected beam size plus space to accommodate the trajectories of both passing and removed bunches. The gap was further increased by $\sim 20\%$ while limiting the entrance and exit apertures of the kicker with electrodes exclusively dedicated to protection of the kicker structure from irradiation by the beam. The kickers need to fit between the quadrupole triplets (650 mm flange-to-flange), which in turn defined the length of the deflecting plates, 0.5 m. To achieve the required separation, the deflection is provided by two kickers placed at $\sim 180^\circ$ betatron phase advance between them. The absorber follows the last kicker with an additional $\sim 90^\circ$ phase advance.

To decrease the power density of the removed bunches at the absorber surface, it is positioned at a small angle with respect to the beam. To keep the distances between the focusing elements constant through the MEBT, the length of the absorber surface is also 0.5 m. Both absorber

* This manuscript has been authored by Fermi Research Alliance, LLC under Contract No. DE-AC02-07CH11359 with the U.S. Department of Energy, Office of Science, Office of High Energy Physics

[†]shemyakin@fnal.gov

and kickers were originally specified and designed to be CW-capable. Some of the parameters of the chopping system elements are presented in Table 1, and the vertical envelopes of the passing and removed bunches simulated for the PIP-II are shown in Fig. 1.

Table 1: Parameters of the Chopper Elements

Parameter	Value	Units
Kicker deflection angle*	7.4	mrad
Gap between kicker plates	16	mm
Gap in the kicker protection electrode	13	mm
Kicker plate length	500	mm
Maximum power from beam loss, CW	40	W
Maximum accidental beam loss	20	J
Absorber surface length	500	mm
Maximum power at absorber, CW	21	kW

* Deflection angle is defined as the angle between passed and removed trajectories created by one kicker.

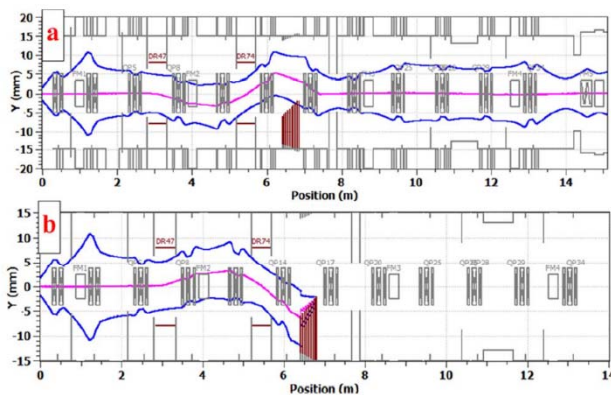


Figure 1: 3σ vertical envelope simulated with Tracewin [4] showing passing (a) and removed (b) trajectories.

KICKERS

Two versions of the kicker and driver, referred below by their impedance, 50 and 200 Ohm, were developed [5] and tested with beam.

50 Ohm Version

The 50-Ohm kicker consists of two identical structures shown in Fig. 2. The beam is deflected by voltage applied to 25 planar electrodes connected in vacuum by coaxial cables with the length determined by necessary delays. Cooling of the Teflon-insulated cables is provided by clamps, which, in turn, are cooled by water flowing through the channels in the structure. The low-power RF measurements showed the excellent agreement with the specified phase velocity (20.08 mm/ns) and low dispersion.

The kicker was expected to be driven by two 0.7 kW CW wideband (0.05 – 1 GHz) linear amplifiers produced by industry. To decrease the low frequency content of the output signal, the 6.15 ns pulse affecting an individual bunch is formed bipolar with zero average voltage. Effects from non-linearities of the amplifier, imperfections of its frequency response and dispersion in cables and the

kicker structure are corrected by pre-distorting the driving signal (see details of proof-of-principle test in [5]).

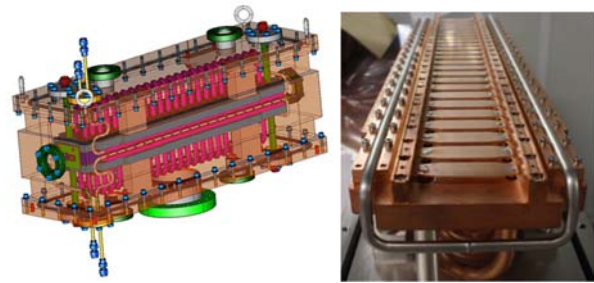


Figure 2: 50-Ohm kicker structure: 3D model and one assembled plate.

Due to budgetary constraints, such amplifiers were not acquired, and the beam tests were performed with the kicker driven by a pair of power amplifiers operating at 81.25 MHz. In this mode, the neighbouring bunches were deflected in opposite directions by ± 250 V on each plate.

The same amplifiers were used to test the thermal characteristics of the kicker. The kickers were subjected to the total power of 2.8 kW CW (374 V per plate) for ~ 100 hours with no changes observed and vacuum at the end $< 10^{-7}$ Torr. The insertion loss during these tests was 0.27 dB.

200 Ohm Version

The travelling wave structure of the 200 Ohm kicker is composed of two helices each with 47 welded plates facing the beam (Fig. 3). Its detailed description can be found in Ref. [6].



Figure 3: Photo of the fully assembled 200 Ohm kicker's two-helix structure.

The high characteristic impedance enables using a fast switch to generate the voltage waveform at the kicker electrodes. As reported in Ref. [6], two prototype switch drivers used in the beam tests are capable of switching the plate voltage between zero and 500 V in 4 ns at rates up to the maximum interesting rate of 81.25 MHz, corresponding to the deflection of every other bunch. The limit for the combination of the macro-pulse length and switching frequency is determined by the heat removal from the switch transistors. The present version with the transistors mounted on G10 and cooled by forced air is limited to CW average switching rate of 500 kHz.

While the RF loss in the structure is low (~ 8 W per helix), the possibility of uncontrolled beam loss of up to 40

Content from this work may be used under the terms of the CC BY 3.0 licence (© 2018). Any distribution of this work must maintain attribution to the author(s), title of the work, publisher, and DOI.

W was foreseen. To ensure the kicker's survival in this scenario, it was subjected to a thermal test, in which a DC current was injected, corresponding to 40 W deposited in each helix. No dramatic vacuum degradation or changes in kicker characteristics were observed.

ABSORBER

The absorber concept [7] features a grazing angle of incidence (29mrad) that decreases the peak power density absorbed at the surface to 17 W/mm²; longitudinal segmentation to relieve thermally-induced stresses; and the molybdenum alloy TZM for the absorbing surface.

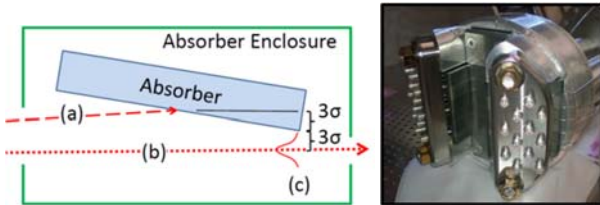


Figure 4: Left: separation scheme with (a) removed beam, (b) passing beam, (c) 6σ shift between two trajectories. Right: photo of the absorber prototype.

Two ¼ length prototypes were manufactured and tested with an electron beam at a dedicated test stand [7]. In part, the second prototype, shown in Fig. 4 (right) photo successfully went through a thermocycle test with more than 10⁴ “30s on- 30s off” cycles at the power density deposited by the electron beam exceeding the level expected for the PIP2IT full – size absorber. This prototype was installed into PIP2IT downstream of the kickers.

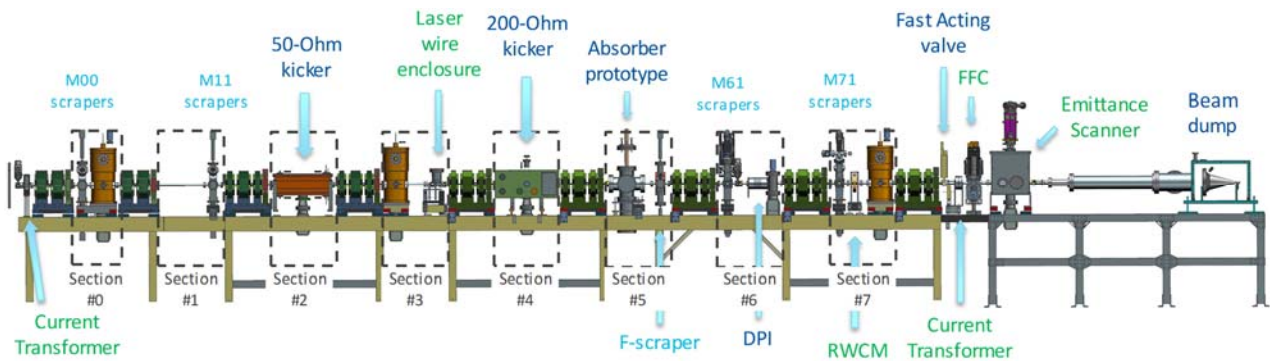


Figure 5: Medium Energy Beam Transport line (side view)

Current transformers are located at the beginning and end of the MEBT; the beam current can be measured from the beam dump as well. An emittance scanner was used to record the vertical beam phase portraits, and a Resistive Wall Current Monitor (RWCM) provided information about the population of the bunches.

TESTS AND RESULTS

Kicker Deflection

Deflection of both kickers was characterized in the MEBT configuration before installation of the DPI, which allowed transporting both “passing” and “removed”

PIP2IT WARM FRONT END

Beam tests of the chopper elements prototypes were performed at the PIP2IT, which presently consists of a 30 kV H⁻ ion source, a LEBT, a 2.1 MeV RFQ capable of accelerating up to 10 mA CW beam, a 10-m long MEBT where the chopper elements are located, and a beam dump [8].

The MEBT (Fig. 5) is a succession of nine “sections” (650-mm long flange-to-flange for sections #1 through #7, and 480 mm for section #0), delimited by transverse focusing assemblies, two quadrupole doublets and 7 triplets. Each group includes a Beam Position Monitor (BPM), whose capacitive pickup is bolted to the poles of one of the quadrupoles. Longitudinal focusing is provided by 3 bunching cavities. The kicker and absorber prototypes are installed in sections 2,4, and 5. In the MEBT configuration shown in Fig. 5, the absorber prototype is followed by a Differential Pumping Insert (DPI). This 200 mm (L) × 10 mm (ID) beam pipe reduces the flux of gas released from the bombardment of the absorber with H⁻ ions into the future cryomodules downstream.

Movable scrapers [9] installed with the main goal to protect the cryomodules against an errant beam or halo were also used to measure the beam size. Shown in Fig. 5 are 4 sets of 4 scrapers (each set consists of a bottom, top, right and left scraper) plus a temporary set of two scrapers (a.k.a. F-scraper, top and right), which was extensively used to characterize the kickers performance.

trajectories to the beam dump with low losses. An Arbitrary Waveform Generator [6] drove the kicker to deflect every other bunch. Then the vertical F-scraper was moved in, and the dump current was recorded as a function of the scraper position. If the two trajectories are well separated, the scan shows two ‘steps’ (Fig. 6).

Quantitatively, the scraper profiles are fitted with a function corresponding to the sum of 2 Gaussian 1D profiles, where the fitting parameters are the mean value of each Gaussian and σ_y , which is assumed to be the same for bunches belonging to either trajectory. The difference between the 2 mean values is the bunch separation. From this, both the optimum phase of the kicker w.r.t. the beam

and the deflection angle at the kicker exit can be inferred. To have good separation and good transmission of both trajectories to the dump, the beam is heavily scraped off in the vertical direction with two scraping stations upstream of the chopper, producing a flat beam.

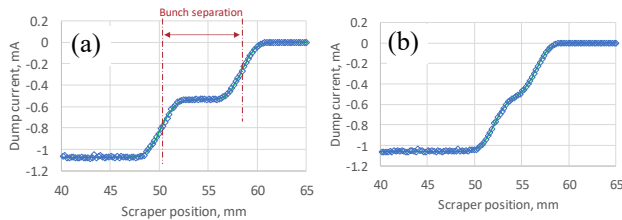


Figure 6: F-scrapers profiles for different delays between the phase of the beam and the 50 Ohm kicker's. (a) Optimum delay; (b) Shifted by 1.73 ns w.r.t. the optimum delay. The beam current after scraping is 1.1 mA (5 mA initially). The fitted rms beam size is 1.15 mm, and the bunch separation is 8.2 mm (a) and 4.4 mm (b).

Routine phasing of the kickers uses the BPM immediately downstream of the F-scrapers. A fast scope records the differential signal from the BPM vertical plates and calculates the difference between peaks of the signals from neighbouring bunches. The kicker delay is varied until this difference is maximized. However, for numerical characterization, the procedure using the F-scrapers (Fig. 6) is employed. The bunch separation plotted as a function of the kicker delay represents the temporal shape of the kicker signal smoothed by the finite length of the beam bunches (Fig. 7).

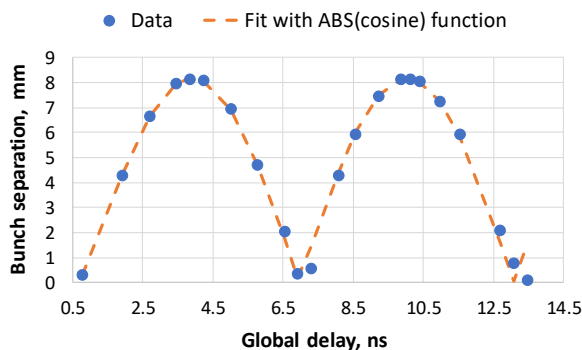


Figure 7: Example of phasing delay of the 50 Ohm kickers with scraper scans.

Using the optical model of the beam line [10], the maximum spatial separation between bunches measured with the F-scrapers is translated into the amplitude of the angular deflection by the kicker. The error of this reconstruction is estimated to do not exceed 5%. In some measurements with the 50 Ohm kicker, there was a significant scatter (~5%) of deflections, likely related to drifts of the kicker's power amplifiers. Within these errors, the measured deflections were in a good agreement with the expected values (7.4 mrad for 500 V plate voltage change).

200 Ohm Version Tests

Several additional tests were performed with the 200 Ohm kicker. One of them is an estimate of the perturbation passing bunches experience. The kicker voltage does not exactly reach the ground potential when the passing bunch arrives, and the bunch centroid undergoes a small deflection. This deflection was measured using the flat beam with the sequence of deflecting every other bunch ("81.25 MHz") and intercepting the removed bunches. The trajectory of the passing bunches was recorded with BPMs and compared to the trajectory with the kicker off. The resulting deflection at nominal parameters was found to be 0.3 mrad, which for the nominal beam creates an emittance dilution of <5%. Note that the average deflection is expected to be lower for other patterns of bunch removal.

Another test is a verification that a difference between the nominal velocity of ions and the phase velocity of the kicker does not affect the deflection amplitude. In these measurements, the phase and amplitude of bunching cavity #2 are changed such as to keep focusing constant but the energy is varied by ± 87 keV. The energy change is then verified from changes of the phases of the downstream BPMs, and the bunch separation is measured at the kicker delay optimum for each energy, E . While one of the points measured is unexplainably shifted, the main effect appears to be a decrease of the deflection with energy as $1/E$, as it would be in the case of a perfect match, and the contribution of a velocity mismatch to the maximum deflection is less than 5% (Fig. 8). Note that if the main goal of the measurement were to compare the kicker phase and ions velocity, a measurement at the rising or falling edges rather than at the maximum would have a better sensitivity to the velocity mismatch.

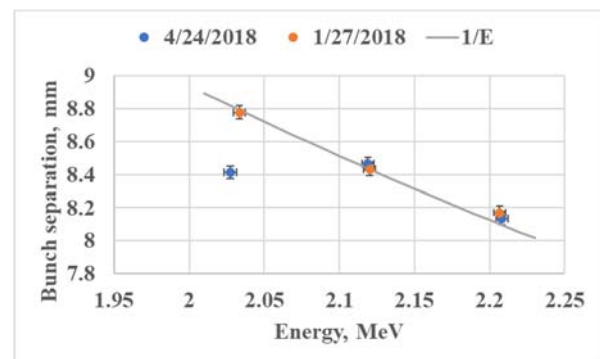


Figure 8: dependence of the bunch separation measured with the F-scrapers on the beam energy. Two sets are measured at different voltage of the kicker plate power supply, with separation scaled to 500 V. The solid curve is $1/E$ dependence drawn through the point measured at the nominal energy.

The 200 Ohm kicker driver in combination with the flat beam and partial insertion of the F-scrapers allows forming arbitrary bunch sequences. Several examples were implemented and recorded with the RWCM: 81.25 MHz

Content from this work may be used under the terms of the CC BY 3.0 licence (© 2018). Any distribution of this work must maintain attribution to the author(s), title of the work, publisher, and DOI.

(already mentioned); a pattern with randomly selected passing and removed bunches; one pattern suitable for the Mu2e experiment (repeatable pattern of 200 ns of passing bunches followed by 1.6 μ s of removed bunches); and aperiodic sequence envisioned for Booster injection. The latter pattern lasted for 0.55 ms macro-pulses, the entire length of the Booster injection (Fig. 9).

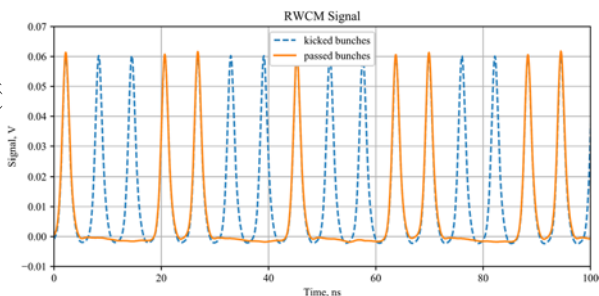


Figure 9: Part of the RWCM signal recording the 0.55 ms Booster injection sequence (orange), superimposed over the signal when the kicker is off (blue). 1.1 mA flat beam.

To test survival of both the driver and the kicker structure for extended operation, the beam was run for 24 hours (with 95% beam availability) at parameters expected for Booster injection [1] 5 mA \times 0.55 ms \times 2.1 MeV \times 20 Hz with the kicker pulsing as depicted in Fig. 9. In addition, a higher-power beam, up to 5 kW, was passed through both (non-pulsing) kickers. No problems were observed even with multiple interruptions induced by the beam touching the kickers. Thus, the Machine Protection System monitoring of the kicker protection electrodes' currents protected the kickers effectively.

Two Kickers Working Together

Preliminary tests were performed with two kickers operating in sync with the 81.25 MHz pattern. The first test was a sanity check, where the kickers, phased individually in advance, were deflecting the flat beam. The total deflection, estimated by the scope signal from the downstream BPM, was equal to the sum of deflections by each kicker. Note that more accurate measurements with F-scraper scans (as in Fig. 6) cannot be performed in this case because the separation is too large to transport both trajectories to the dump with low losses.

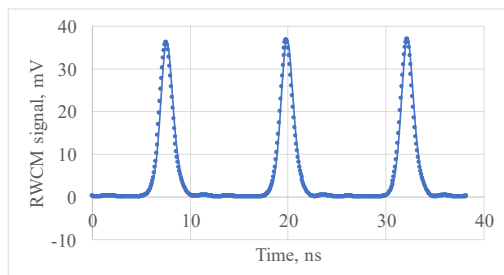


Figure 10: RWCM signal of an initially 5 mA beam with two kickers operating synchronously at 81.25 MHz.

The second test was performed with a full-intensity beam to mimic operation in a high-power mode, though the pulse length was still 10 μ s. The scrapers upstream of the chopping system were moved to the beam boundary as they were during high-power runs, intercepting \sim 1% of the beam current. After careful tuning with dipole correctors through the tight apertures of the pulsing kickers, the beam losses to their protection electrodes were decreased to below 10 μ A each, which, according to previous measurements, ensures that the loss power to the kickers stays well below the specified 40 W.

Then the F-scraper was moved in to the position where the beam current to the dump dropped by a factor of two in comparison with the case of the kickers being turned off. The RWCM signal showed that the intensity of the removed bunches dropped below 2% of the passing ones (Fig. 10).

Absorber Prototype

While time limitations did not allow to test the absorber prototype with the highest power available, it was irradiated for 36 hours with 98% beam up-time with the following parameters: 1.75 ms \times 20 Hz \times 10 mA \times 2.1 MeV = 735 W (with the kickers off). No damage or deterioration was observed.

Tuning of the beam position at the absorber surface was expected and initially made using thermocouples squeezed between the TZM bricks forming the absorbing surface. A surprising help came from imaging of the surface with a camera in the visible spectrum. Even though the surface was not hot enough for thermal radiation, and the OTR light should be too faint to be observed, a bright light clearly indicated the beam position at the absorber surface (Fig. 11). The present speculation is that it is related to poor vacuum in the time of the measurements (up to $6 \cdot 10^{-6}$ Torr) because no pumping had been installed yet.

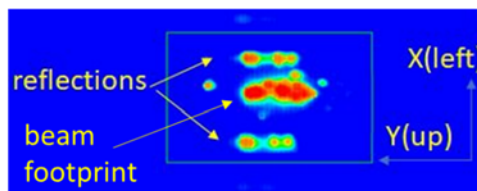


Figure 11: Fi Image, in false colors, of the beam footprint at the absorber surface. Side traces are reflections from the absorber walls. The length of the footprint (along the beam axis) is \sim 40 mm. 3 ms \times 20 Hz \times 10 mA.

SUMMARY AND PLANS

Prototypes of two kicker variants and of the absorber were successfully tested with a 2.1 MeV H⁻ beam at PIP2IT. The 200 Ohm kicker version demonstrated all capabilities required for PIP-II operation with bucket-to-bucket injection to Booster. A full-size absorber is being manufactured, and production of two kickers and their drivers (200 Ohm version) is expected in 2019. When PIP2IT operation resumes after installation of the cryomodules, the chopping system will demonstrate being

able to deliver a beam with nominal parameters chopped according to the Booster injection requirements.

ACKNOWLEDGMENT

The authors are thankful to the many people who contributed to building the prototype chopping system and helped with the measurements, including B. Fellenz, D. Franck, M. Hassan, S. Khole, D. Lambert, W. Mueller, R. Neswold, D. Nicklaus, A. Saewert, V. Scarpine, J. Simmons, R. Thurman-Keup.

REFERENCES

- [1] PIP-II Conceptual Design Report (2017); <http://pip2-docdb.fnal.gov/cgi-bin/ShowDocument/docid=113>
- [2] Project X Reference Design Report (2013); <http://projectx-docdb.fnal.gov/cgi-bin/ShowDocuent/docid=776>
- [3] P. F. Derwent *et al.*, “PIP-II Injector Test: challenges and status”, in *Proc. LINAC'16*, East Lansing, MI, USA, 2016, paper WE1A01, pp. 641-645.
- [4] TraceWin code, <http://irfu.cea.fr/Sacm/logiciels/>
- [5] V. Lebedev *et al.*, “Progress with PXIE MEBT chopper”, in *Proc. IPAC'12*, New Orleans, LA, USA, 2012, paper WEPD078.
- [6] G. Saewert *et al.*, “First Performance results of the PIP2IT MEBT 200-Ohm kicker prototype”, in *Proc. IPAC'18*, Vancouver, BC, Canada, 2018, paper WEPML021.
- [7] A. Shemyakin and C. Baffes, “High power density test of PXIE MEBT absorber prototype”, in *Proc. LINAC'14*, Geneva, Switzerland, 2014, paper THPP055.
- [8] L.R. Prost, R. Andrews, C.M. Baffes, J.-P. Carneiro, B.E. Chase, A.Z. Chen, E. Cullerton, P. Derwent, J.P. Edelen, J. Einstein-Curtis, D. Frolov, B.M. Hanna, D.W. Peterson, G.W. Saewert, A. Saini, V.E. Scarpine, A.V. Shemyakin, V.L. Sista, J. Steimel, D. Sun, A. Warner, C.J. Richard, V.L. Sista, “PIP-II Injector Test Warm Front End: Commissioning Update”, in *Proc. IPAC'18*, Vancouver, Canada, 2018, paper THYGBF2.
- [9] A. Saini and A. Shemyakin, “Optical design of the PI-Test MEBT beam scraping system”, in *Proc. LINAC'16*, East Lansing, MI, USA, 2016, paper THPRC026.
- [10] A. Shemyakin, J.-P. Carneiro, B. Hanna, V. Lebedev, L. Prost, A. Saini, V. Scarpine, V.L. Sista, C. Richard, “Experimental study of beam dynamics in the PIP-II MEBT prototype”, presented at HB'18, Daejeon, Korea, June 2018, paper MOP1WB03, this conference.